Electronic Supplementary Information for

Flexible synthesis of Au@Pd core-shell mesoporous nanoflowers for efficient methanol oxidation

Shuli Yin, Ziqiang Wang,* Songliang Liu, Shiqian Jiao, Wenjing Tian, You Xu, Xiaonian Li, Liang Wang* and Hongjing Wang *

State Key Laboratory Breeding Base of Green-Chemical Synthesis Technology, College of Chemical Engineering, Zhejiang University of Technology, Hangzhou 310014, P.R. China.

E-mails: zqwang@zjut.edu.cn; wangliang@zjut.edu.cn; hjw@zjut.edu.cn

Characterization

The particle size and morphology of the samples were characterized by ZEISS Gemini 500 scanning electron microscope (SEM) operated at 5 kV. Transmission electron microscopy (TEM), and high-resolution TEM (HRTEM) were performed with a TalosS-FEG operated at 200 kV. The phase and crystallinity of the samples were studied by X-ray diffraction (XRD, PANalytical X'Pert Powder) using Cu Ka radiation. X-ray photoelectron spectroscopy (XPS) measurements were conducted on the Thermo escalab 250Xi instrument using Al *Kα* radiation (*hv* = 1486.6 eV) operated at 150 W.

Electrochemical measurements of the MOR

A CHI 660E electrochemical analyzer was used to measure the electrochemical performance. A traditional three-electrode cell including a working electrode (modified glassy carbon electrode), a counter electrode (Pt wire) and a reference electrode (Ag/AgCl electrode (3 M KCl)) was used. For the modification of the working electrode, 10 μg of the catalyst was dropped on the surface of a clean glassy carbon electrode, followed by drying at 323 K. Then 3 μL of Nafion (0.5%) was coated and left to dry at the same temperature. The current densities are normalized by the electrode area (0.071 cm^2). The electrochemically active surface area (ECSA) of the catalyst was calculated from the area in the reduction peak of the Pd oxide using the following equation: ECSA = Q/(m×*q)*, where Q is the surface charge for oxygen desorption, m is the metal loading and *q* is the charge of desorbing a monolayer of oxygen on the Pd surface (424 μC cm^{-2}). MOR investigations were conducted in 1 M KOH with 1 M CH_3OH electrolyte at a scan rate of 50 mV s^{-1}.

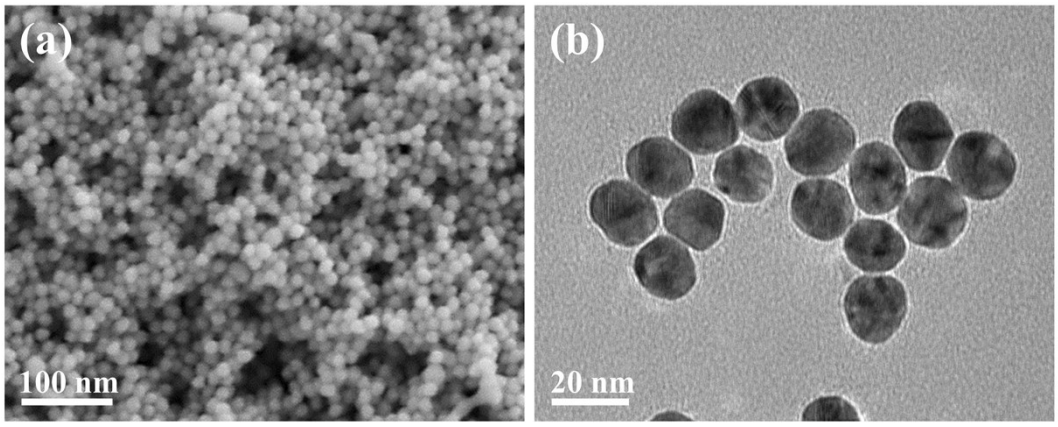

Fig. S1 (a, b) SEM and TEM images of the Au nanoparticles.

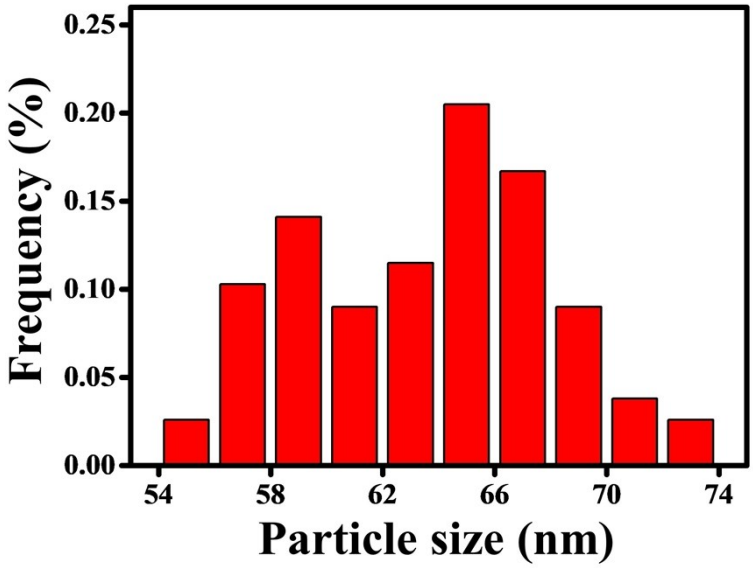

Fig. S2 Size distribution histogram of the Au@mPd NFs.

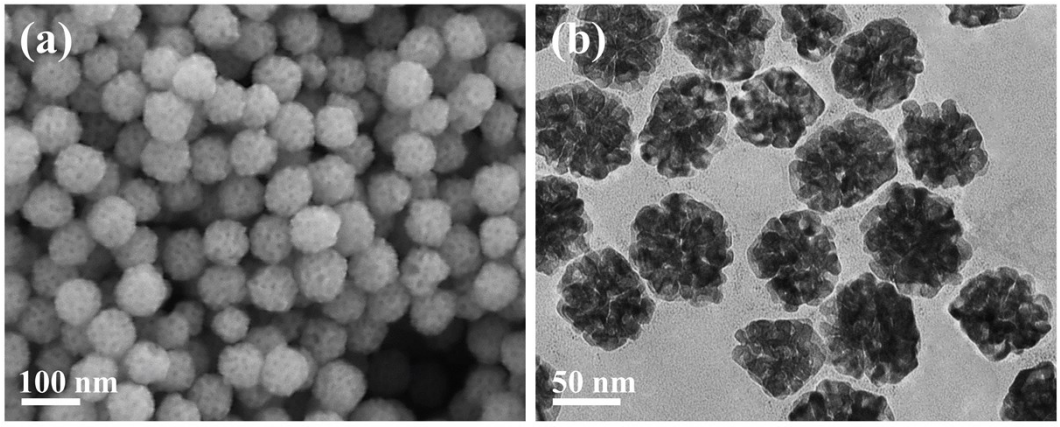

Fig. S3 (a, b) SEM and TEM images of the mPd NFs.

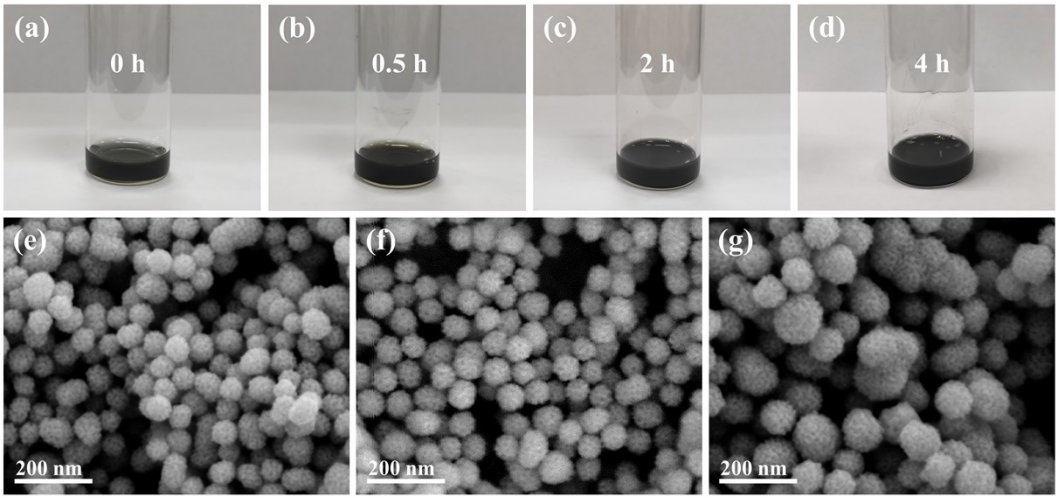

Fig. S4 (a-d) Photographs of the colloidal suspensions of reaction solutions at different reaction times. (e-g) SEM images of Au@mPd NFs prepared from different reaction times: (e) 0.5 h, (f) 2 h and (g) 4 h.

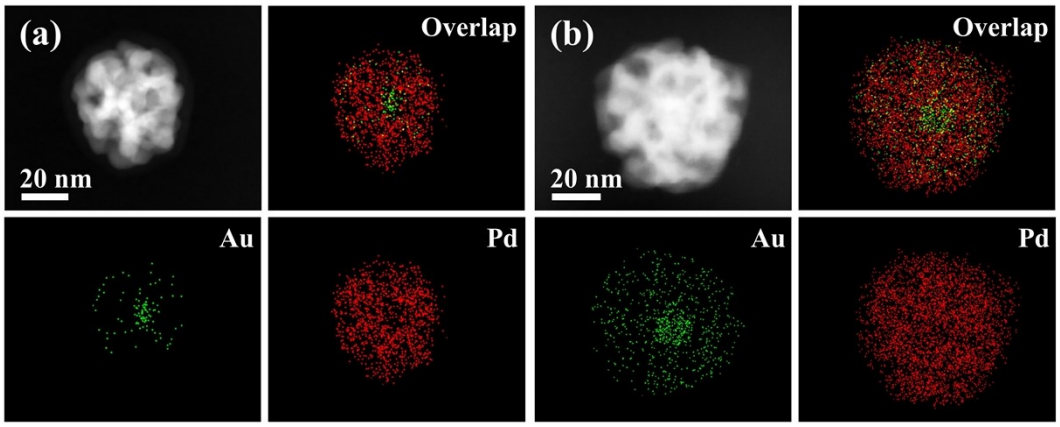

Fig. S5 HAADF-STEM images and elemental mapping images of Au@mPd NFs prepared from different reaction times: (a) 0.5 h and (b) 4 h.

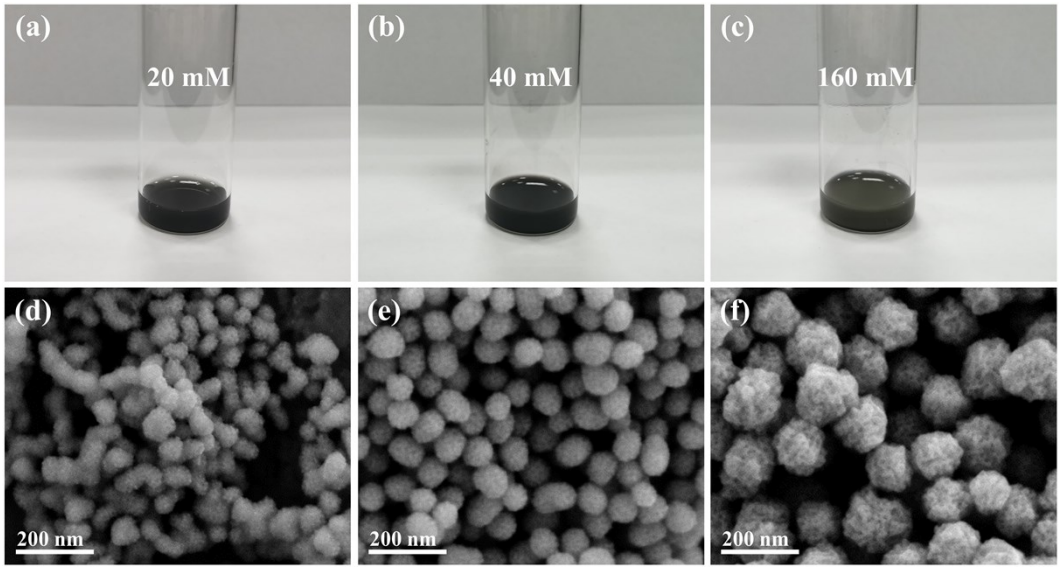

Fig. S6 (a-c) Photographs of the colloidal suspensions of reaction solutions with different concentration of precursor. (d-f) SEM images of Au@mPd NFs from different concentration of precursor: (d) 20, (e) 40 and (f) 160 mM.

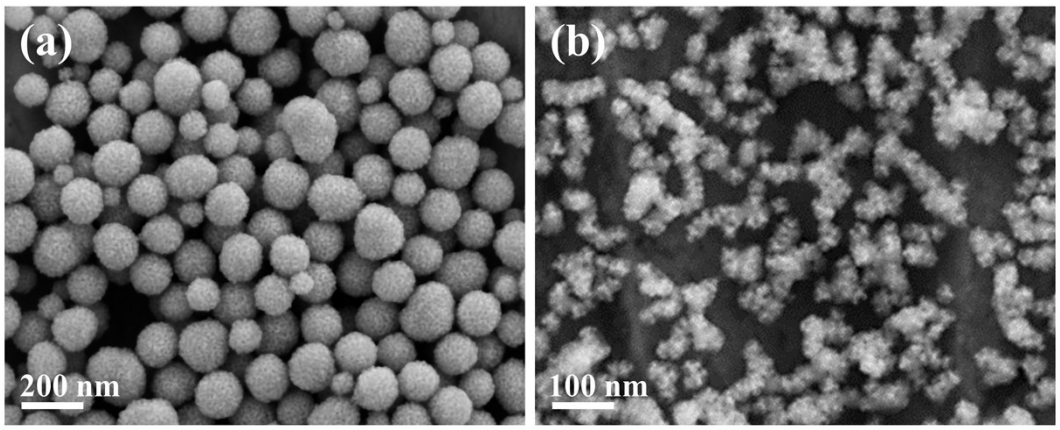

Fig. S7 SEM images of the samples prepared with different amount of Au nanoparticles: (a) 10 μL and (b) 200 μL.

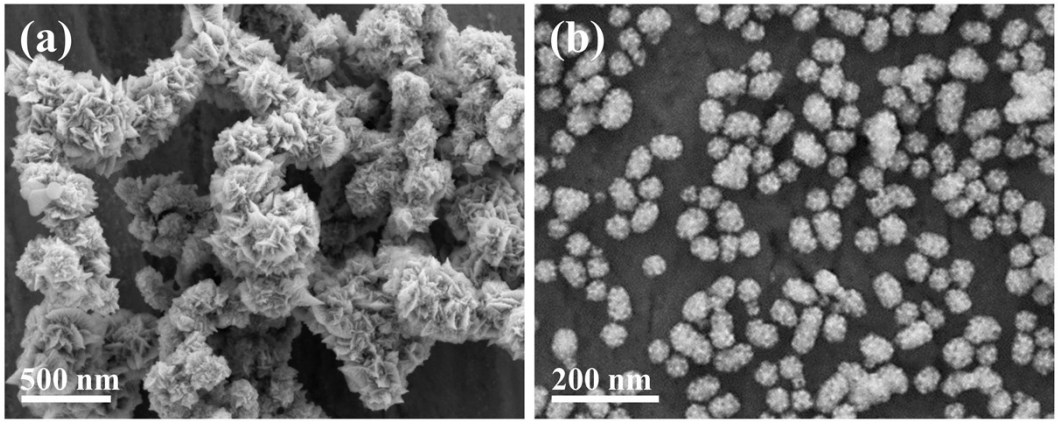

Fig. S8 SEM images of the samples prepared without (a) PS-b-PEO and (b) HCl.

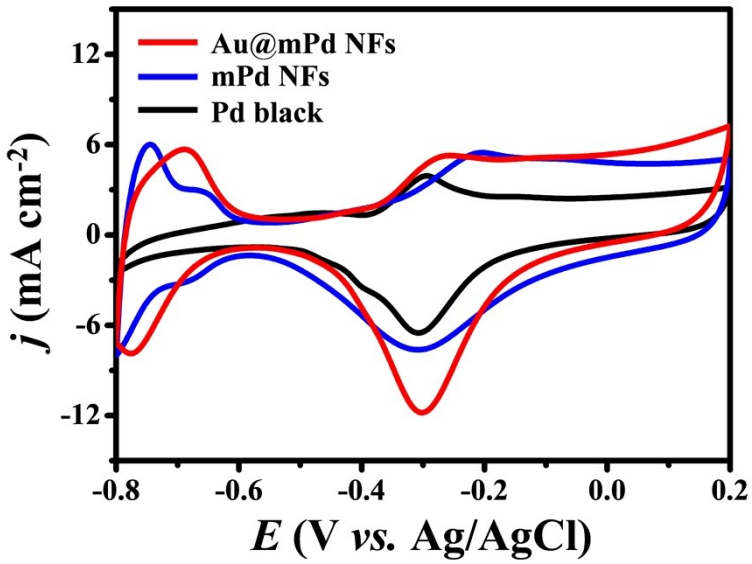

Fig. S9 CV curves of the different catalysts.

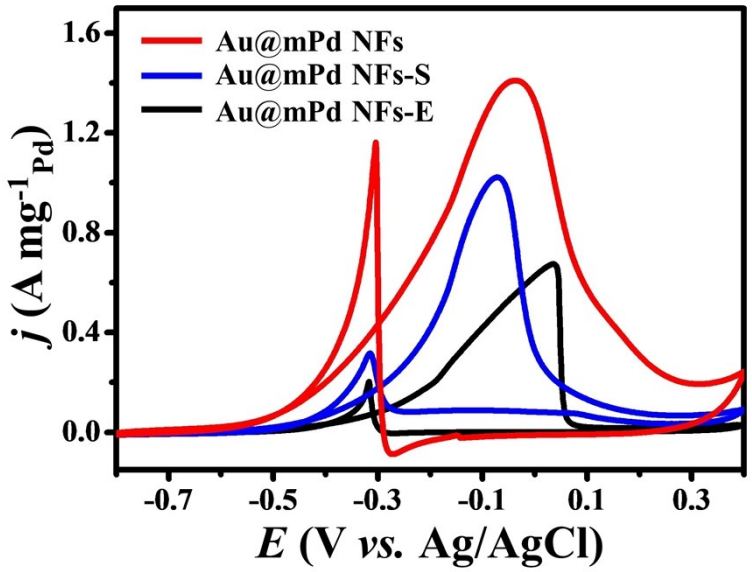

Fig. S10 Mass-normalized CV curves of different catalysts.

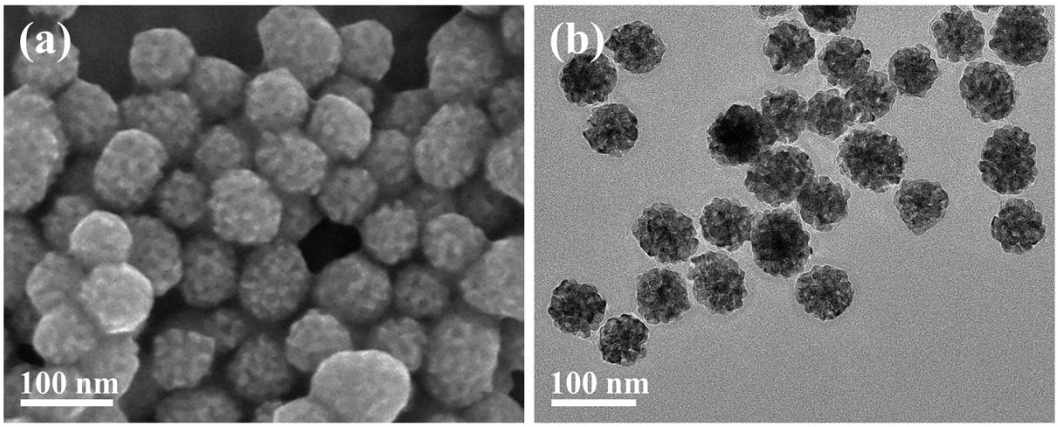

Fig. S11 (a, b) SEM and TEM images of Au@mPd NFs after stability test.

Table S1. The specific activity and mass activity comparisons of MOR on various Pd-based electrocatalysts.

Catalyst	**specific activity ($mA\ cm^{-2}$)**	**mass activity ($mA\ \mu g^{-1}_{Pd}$)**	**Ref.**
Au@mPd NFs	**4.57**	**1.41**	**This work**
Bowl-like PdCu	3.32	1.46	1
PdCuCo / RGO	0.92	1.06	2
$Pd_{78}Co_{22}$	2.76	1.48	3
PdGa NSAs	1.10	2.65	4
Pd_3Rh_1	4.00	0.44	5
echinus-like PdCu NCs	2.76	1.2021	6
flower-like Pd particles	2.39	/	7
Pd-4Er/C catalyst	2.09	/	8

References

1 S.-Q. Liu, Y.-T. Xu, J.-Q. Xie, G.-Q. Sheng, Y.-W. Zhu, X.-Z. Fu, R. Sun and C.-P. Wong, *ACS Appl. Energy Mater.*, 2018, **1**, 3323-3330.

2 F. Yang, B. Zhang, S. Dong, C. Wang, A. Feng, X. Fan and Y. Li, *J. Energy Chem.*, 2019, **29**, 72-78.

3 G. Sheng, J. Chen, H. Ye, Z. Hu, X.-Z. Fu, R. Sun, W. Huang and C.-P. Wong, *J. Colloid Interface Sci.*, 2018, **522**, 264-271.

4 H. Shang, H. Xu, C. Wang, L. Jin, C. Chen, G. Zhou, Y. Wang and Y. Du, *Nanoscale*, 2020, **12**, 3411-3417.

5 Q.-Y. Hu, R.-H. Zhang, D. Chen, Y.-F. Guo, W. Zhan, L.-M. Luo and X.-W. Zhou, *Int. J. Hydrogen Energy*, 2019, **44**, 16287-16296.

6 Z. Zhang, G. Ren, Y. Liu, Y. Liang, M. Wang, S. Wu and J. Shen, *Chem. Asian J.*, 2019, **14**, 4217-4222.

7 Z. Li, H. Gong, T. Mu and Y. Luan, *CrystEngComm*, 2014, **16**, 4038–4044.

8 D. Hua, L. Y. Zhang, K. Meng, Z. Jia, Y. Wang and T. Qi, *Ionics*, **2020**, 1-6.